Inorg. Chem. **2008**, *47*, 4545−4553

Synthesis, Structure, and Electrocatalysis of Diiron C-Functionalized Propanedithiolate (PDT) Complexes Related to the Active Site of [FeFe]-Hydrogenases

Li-Cheng Song,* Chang-Gong Li, Jie Gao, Bang-Shao Yin, Xiang Luo, Xiao-Guang Zhang, Hai-Lin Bao, and Qing-Mei Hu

Department of Chemistry, State Key Laboratory of Elemento-Organic Chemistry, Nankai University, Tianjin 300071, China

Received October 8, 2007

New C-functionalized propanedithiolate-type model complexes (**1**−**8**) have been synthesized by functional transformation reactions of the known complex $[(\mu\text{-}SCH_2)_2CH(OH)]Fe_2(CO)_6$ (**A**). Treatment of **A** with the acylating agents PhC(O)Cl, 4-pyridinecarboxylic acid chloride, 2-furancarbonyl chloride, and 2-thiophenecarbonyl chloride in the presence of Et_3N affords the expected C-functionalized complexes $[(\mu\text{-}SCH_2)_2CHO_2CPh]Fe_2(CO)_6$ (**1**), $[(\mu\text{-}SCH_2)_2CHO_2CC_5H_4N\text{-}4]Fe_2(CO)_6$ (**2**), $[(\mu\text{-}SCH_2)_2CHO_2CC_4H_3O\text{-}2]Fe_2(CO)_6$ (**3**), and $[(\mu\text{-}SCH_2)_2CHO_2CC_4H_3S\text{-}2]Fe_2(CO)_6$ (**4**). However, when **A** is treated with the phosphatizing agents Ph_2PCl, PCl_3 and PBr_3, both C- and Fe-functionalized complexes $[(\mu\text{-}SCH_2)_2CHOPPh_2\text{-}\eta^1]Fe_2(CO)_5$ (**5**), $[(\mu\text{-}SCH_2)_2CHOPCl_2\text{-}\eta^1]Fe_2(CO)_5$ (**6**), and $[(\mu\text{-}SCH_2)_2CHOPBr_2\text{-}\eta^1]Fe_2(CO)_5$ (**7**) are unexpectedly obtained via intramolecular CO substitution by P atoms of the initially formed phosphite complexes. The simplest C-functionalized model complex $[(\mu\text{-}SCH_2)_2C{=}O]Fe_2(CO)_6$ (**8**) can be produced by oxidation of **A** with Dess−Martin reagent. While **8** is found to be an electrocatalyst for proton reduction to hydrogen, starting complex **A** can be prepared by another method involving the reaction of $HC(OH)(CH_2Br)_2$ with the in situ generated $(\mu\text{-}LiS)_2Fe_2(CO)_6$. X-ray crystallographic studies reveal that the bridgehead C atom of **8** is double-bonded to an O atom to form a ketone functionality, whereas the bridgehead C atoms of **A**, **1**, **3**, and **4** are equatorially-bonded to their functionalities and those of **5**−**7** axially-bonded to their functionalities due to formation of the corresponding P−Fe bond-containing heterocycles.

Introduction

Hydrogenases are a class of natural enzymes that can catalyze H_2 metabolism in several microorganisms.[1,2] According to the metal content, they are generally classified as [FeFe]-hydrogenases, [NiFe]-hydrogenases, and [Fe]-hydrogenases (Hmd).[3,4] Among these types of hydrogenases, [FeFe]-hydrogenases have recently received much more attention than the other two, largely due to their unusual structure and particularly their extremely high capability for production of "clean" and highly efficient hydrogen fuel.[5−8]

Combined studies of X-ray crystallography[9−11] and FTIR spectroscopy[12−14] demonstrated that [FeFe]-hydrogenases contain a structurally uncommon active site (so-called H-cluster), which is composed of a butterfly [2Fe2S] cluster with one of its iron atoms connected to a cubane-like [4Fe4S] cluster via the sulfur atom of a cysteinyl ligand. In addition,

* To whom correspondence should be addressed. E-mail: lcsong@nankai.edu.cn. Fax: 0086-22-23504853.

(1) Cammack, R. *Nature* **1999**, *397*, 214.
(2) Adams, M. W. W.; Stiefel, E. I. *Science* **1998**, *282*, 1842.
(3) Frey, M. *ChemBioChem* **2002**, *3*, 153.
(4) Shima, S.; Thauer, R. K. *Chem. Rec.* **2007**, *7*, 37.
(5) Darensbourg, M. Y.; Lyon, E. J.; Zhao, X.; Georgakaki, I. P. *Proc. Natl. Acad. Sci. U.S.A.* **2003**, *100*, 3683.
(6) Evans, D. J.; Pickett, C. J. *Chem. Soc. Rev.* **2003**, *32*, 268.
(7) Alper, J. *Science* **2003**, *299*, 1686.
(8) Song, L.-C. *Acc. Chem. Res.* **2005**, *38*, 21.
(9) Peters, J. W.; Lanzilotta, W. N.; Lemon, B. J.; Seefeldt, L. C. *Science* **1998**, *282*, 1853.
(10) Nicolet, Y.; Piras, C.; Legrand, P.; Hatchikian, C. E.; Fontecilla-Camps, J. C. *Structure* **1999**, *7*, 13.
(11) Nicolet, Y.; De Lacey, A. L.; Vernède, X.; Fernandez, V. M.; Hatchikian, E. C.; Fontecilla-Camps, J. C. *J. Am. Chem. Soc.* **2001**, *123*, 1596.
(12) Pierik, A. J.; Hulstein, M.; Hagen, W. R.; Albracht, S. P. J. *Eur. J. Biochem.* **1998**, *258*, 572.
(13) De Lacey, A. L.; Stadler, C.; Cavazza, C.; Hatchikian, E. C.; Fernandez, V. M. *J. Am. Chem. Soc.* **2000**, *122*, 11232.
(14) Chen, Z.; Lemon, B. J.; Huang, S.; Swartz, D. J.; Peters, J. W.; Bagley, K. A. *Biochemistry* **2002**, *41*, 2036.

10.1021/ic701982z CCC: $40.75
Published on Web 04/26/2008

Scheme 1

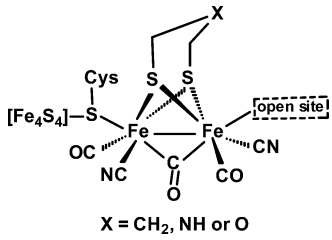

the two iron atoms of the [2Fe2S] cluster are connected to CO and CN^- ligands and are bridged by a dithiolate SCH_2XCH_2S cofactor (Scheme 1). This structural information has encouraged chemists to synthesize a wide variety of H-cluster models.[15–28] Among these models, the C-functionalized propanedithiolate (PDT) and the N-functionalized azadithiolate (ADT) models are of particular interest, since they could be easily modified by functional transformation reactions to get a variety of biomimetic analogues with novel structure and improved catalytic properties.[18,19,26] In this paper, we report the synthesis, structural characterization, and properties of a new series of C-functionalized PDT models obtained by functional transformation reactions of the known complex $[(\mu\text{-}SCH_2)_2CH(OH)]Fe_2(CO)_6$ (**A**).[29] In addition, a new synthetic method for complex **A** and the biomimetic H_2 evolution catalyzed by one of the new models are also described.

Results and Discussion

Synthesis and Characterization of Starting Complex $[(\mu\text{-}SCH_2)_2CH(OH)]Fe_2(CO)_6$ (A). Since 1982, when Huttner first prepared complex **A** by oxidative addition method of $Fe_3(CO)_{12}$ with dithiol $HSCH_2CH(OH)CH_2SH$,[29] no other synthetic method for this complex has been reported. However, we recently found a method by which **A** can be conveniently prepared with a moderate yield. That is, the treatment of $(\mu\text{-}LiS)_2Fe_2(CO)_6$ (prepared from $(\mu\text{-}S_2)Fe_2(CO)_6$ and Et_3BHLi)[30] with 1,3-dibromo-2-propanol resulted in the formation of **A** in 42% yield (Scheme 2). The structure of **A** obtained by this method has been fully characterized by elemental analysis, spectroscopy, and X-ray crystallography. For example, the IR spectrum of **A** showed five absorption bands in the range 2078−1973 cm^{-1} for its terminal carbonyls and one broad band at 3302 cm^{-1} for its hydroxy group. The ^1H NMR spectrum displayed a multiplet around 3.10 ppm for the hydrogen atom attached to its bridgehead C atom, and it displayed a triplet at 1.50 ppm and a doublet/doublet at 2.79 ppm for the axial and the equatorial hydrogens in its two CH_2S groups, respectively. The crystal structure of **A** determined by X-ray diffraction analysis contains 0.5 $CHCl_3$ molecules per molecule of **A**.[31] While Figure 1 shows its ORTEP plot, Table 1 lists its selected bond lengths and angles. As can be seen in Figure 1, complex **A** contains a hydroxylpropanedithiolate ligand, which is bridged between two Fe atoms of the diiron subsite to form two fused six-membered rings Fe1S1C7C8C9S2 and Fe2S1C7C8C9S2. The hydroxyl group and the hydrogen atom attached to the bridgehead C8 atom reside in the common equatorial and axial positions of the above-mentioned chair and boat-shaped six-membered rings, respectively. In addition, the Fe−Fe bond length of our **A** (2.5164 Å) is actually the same as that reported (2.524 Å)[31] and is very close to those reported for similar diiron carbonyl complexes.[23,28,32]

Synthesis and Characterization of Model Complexes $[(\mu\text{-}SCH_2)_2CHO_2CPh]Fe_2(CO)_6$ (1), $[(\mu\text{-}SCH_2)_2CHO_2CC_5H_4N\text{-}4]Fe_2(CO)_6$ (2), $[(\mu\text{-}SCH_2)_2CHO_2CC_4H_3O\text{-}2]Fe_2(CO)_6$ (3), and $[(\mu\text{-}SCH_2)_2CHO_2CC_4H_3S\text{-}2]Fe_2(CO)_6$ (4). The C-functionalized PDT-type models **1**−**4** were prepared via functional transformation reactions of the C-hydroxyl group of complex **A**. Thus, acylation of **A** with benzoyl chloride or 4-pyridinecarboxylic acid chloride in CH_2Cl_2 in the presence of Et_3N gave the expected C-benzoate and C-pyridinecarboxylate complexes **1** and **2** in 63% and 61% yields, respectively, whereas **A** reacted with 2-furancarbonyl chloride or 2-thiophenecarbonyl chloride under similar conditions to afford the corresponding C-furancarboxylate and C-thiophenecarboxylate complexes **3** and **4** in 70% and 58% yields, respectively (Scheme 3).

Complexes **1**−**4** are air-stable red solids, which have been characterized by elemental analysis and spectroscopy. The IR spectra of **1**−**4** displayed five to six absorption bands in the region 2076−1937 cm^{-1} for their terminal carbonyls and one absorption band in the range 1735−1718 cm^{-1} for their ester carbonyls. The ^1H NMR spectra of **1**−**4** showed a broad

(15) Gloaguen, F.; Lawrence, J. D.; Schmidt, M.; Wilson, S. R.; Rauchfuss, T. B. *J. Am. Chem. Soc.* **2001**, *123*, 12518.
(16) Lyon, E. J.; Georgakaki, I. P.; Reibenspies, J. H.; Darensbourg, M. Y. *J. Am. Chem. Soc.* **2001**, *123*, 3268.
(17) Razavet, M.; Davies, S. C.; Hughes, D. L.; Barclay, J. E.; Evans, D. J.; Fairhurst, S. A.; Liu, X.; Pickett, C. J. *Dalton Trans.* **2003**, 586.
(18) Tard, C.; Liu, X.; Ibrahim, S. K.; Bruschi, M.; De Gioia, L.; Davies, S. C.; Yang, X.; Wang, L.-S.; Sawers, G.; Pickett, C. J. *Nature* **2005**, *433*, 610.
(19) Thomas, C. M.; Rüdiger, O.; Liu, T.; Carson, C. E.; Hall, M. B.; Darensbourg, M. Y. *Organometallics* **2007**, *26*, 3976.
(20) Gloaguen, F.; Lawrence, J. D.; Rauchfuss, T. B. *J. Am. Chem. Soc.* **2001**, *123*, 9476.
(21) Capon, J.-F.; Hassnaoui, S. E.; Gloaguen, F.; Schollhammer, P.; Talarmin, J. *Organometallics* **2005**, *24*, 2020.
(22) Adam, F. I.; Hogarth, G.; Richards, I.; Sanchez, B. E. *Dalton Trans.* **2007**, 2495.
(23) Lawrence, J. D.; Li, H.; Rauchfuss, T. B. *Chem. Commun.* **2001**, 1482.
(24) Lawrence, J. D.; Li, H.; Rauchfuss, T. B.; Bénard, M.; Rohmer, M.-M. *Angew. Chem., Int. Ed.* **2001**, *40*, 1768.
(25) Song, L.-C.; Ge, J.-H.; Zhang, X.-G.; Liu, Y.; Hu, Q.-M. *Eur. J. Inorg. Chem.* **2006**, 3204.
(26) (a) Song, L.-C.; Tang, M.-Y.; Su, F.-H.; Hu, Q.-M. *Angew. Chem., Int. Ed.* **2006**, *45*, 1130. (b) Song, L.-C.; Tang, M.-Y.; Mei, S.-Z.; Huang, J.-H.; Hu, Q.-M. *Organometallics* **2007**, *26*, 1575.
(27) Song, L.-C.; Yang, Z.-Y.; Bian, H.-Z.; Liu, Y.; Wang, H.-T.; Liu, X.-F.; Hu, Q.-M. *Organometallics* **2005**, *24*, 6126.
(28) (a) Song, L.-C.; Yang, Z.-Y.; Hua, Y.-J.; Wang, H.-T.; Liu, Y.; Hu, Q.-M. *Organometallics* **2007**, *26*, 2106. (b) Song, L.-C.; Yin, B.-S.; Li, Y.-L.; Zhao, L.-Q.; Ge, J.-H.; Yang, Z.-Y.; Hu, Q.-M. *Organometallics* **2007**, *26*, 4921.
(29) Winter, A.; Zsolnai, L.; Huttner, G. *Z. Naturforsch., B: Anorg. Chem., Org. Chem.* **1982**, *37*, 1430.
(30) Seyferth, D.; Henderson, R. S.; Song, L.-C. *J. Organomet. Chem.* **1980**, *192*, C1.
(31) During the review of this submission another crystal structure of **A** with 0.5 CH_2Cl_2 was reported, see: Apfel, U.-P.; Halpin, Y.; Görls, H.; Vos, J. G.; Schweizer, B.; Linti, G.; Weigand, W. *Chem. Biodivers.* **2007**, *4*, 2138.
(32) Lyon, E. J.; Georgakaki, I. P.; Reibenspies, J. H.; Darensbourg, M. Y. *Angew. Chem., Int. Ed.* **1999**, *38*, 3178.

Scheme 2

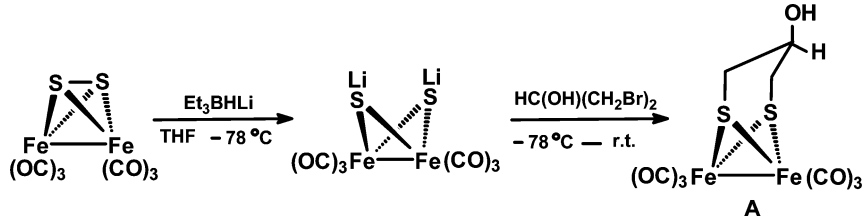

singlet or a multiplet around 4.50 ppm for their bridgehead C-attached axial hydrogen atoms, and they showed a triplet at approximately 1.70 ppm and a doublet/doublet or simply a doublet at approximately 2.90 ppm for the axial and equatorial hydrogens in their two CH_2S groups.

The molecular structures of **1**, **3**, and **4** were unambiguously confirmed by X-ray diffraction techniques (Figures 2–4 and Table 1). As can be seen intuitively from Figures 2–4, complexes **1**, **3**, and **4** much resemble complex **A** containing a benzoate, a furancarboxylate, or a thiophenecarboxylate functionality equatorially attached to the bridgehead C8 atom of the corresponding two fused six-membered rings, and the hydrogen atom attached to the bridgehead C8 is in the axial position of the two fused six-membered rings. The Fe−Fe bond lengths of **1**, **3**, and **4** (2.4973−2.5088 Å) are very close to those of **A** and the analogous diiron dithiolate complexes.[23,28,32]

Synthesis and Characterization of Model Complexes [(μ-SCH$_2$)$_2$CHOPPh$_2$-η^1]Fe$_2$(CO)$_5$ (5), [(μ-SCH$_2$)$_2$-CHOPCl$_2$-η^1]Fe$_2$(CO)$_5$ (6), [(μ-SCH$_2$)$_2$CHOPBr$_2$-η^1]Fe$_2$(CO)$_5$ (7), and [(μ-SCH$_2$)$_2$C=O]Fe$_2$(CO)$_6$ (8). The C-functionalized PDT-type models **5**−**8** could also be prepared by functional transformation reactions of complex **A**. The C-diphenylphosphite complex **5**, in which its P atom is coordinated to one Fe atom of the diiron subsite, was unexpectedly produced by the reaction of **A** with Ph_2PCl in the presence of Et_3N in 48% yield; this reaction is most likely to proceed via intermolecular condensation of **A** with the phosphatizing agent Ph_2PCl to give the initially formed phosphite complex $\mathbf{M_1}$ and then the intramolecular CO substitution of $\mathbf{M_1}$ by its P atom (Scheme 4). As the analogues of **5**, dichloro- and dibromophosphite complexes **6** and **7** were similarly prepared in approximately 73% yield by condensation of **A** with PX_3 to give intermediates $\mathbf{M_2}$ and $\mathbf{M_3}$ followed by intramolecular CO substitution of these intermediates by their P atoms (Scheme 4). The bridgehead C=O functionality-containing model complex **8** was obtained in 40% yield by oxidation of the bridgehead C-hydroxyl group using Dess−Martin reagent (periodinane) (Scheme 4).[33]

Table 1. Selected Bond Lengths (Å) and Angles (deg) for **A**, **1**, **3**, and **4**

		A	
Fe(1)−S(1)	2.258(2)	Fe(2)−S(2)	2.266(2)
Fe(1)−S(2)	2.263(2)	C(7)−C(8)	1.481(8)
Fe(1)−Fe(2)	2.5164(14)	C(8)−C(9)	1.433(8)
Fe(2)−S(1)	2.2582(19)	O(7)−C(8)	1.427(7)
S(1)−Fe(1)−S(2)	85.30(7)	S(1)−Fe(2)−Fe(1)	56.14(5)
S(1)−Fe(1)−Fe(2)	56.14(5)	S(2)−Fe(2)−Fe(1)	56.20(6)
S(2)−Fe(1)−Fe(2)	56.30(6)	Fe(2)−S(1)−Fe(1)	67.72(6)
S(1)−Fe(2)−S(2)	85.24(7)	C(9)−C(8)−C(7)	119.7(7)
		1	
Fe(1)−S(1)	2.2401(11)	Fe(2)−S(2)	2.2527(11)
Fe(1)−S(2)	2.2416(10)	C(7)−C(8)	1.500(4)
Fe(1)−Fe(2)	2.4973(8)	C(8)−C(9)	1.502(4)
Fe(2)−S(1)	2.2481(11)	O(7)−C(8)	1.453(4)
S(1)−Fe(1)−S(2)	85.51(3)	Fe(1)−S(2)−Fe(2)	67.51(3)
S(1)−Fe(1)−Fe(2)	56.34(3)	S(1)−Fe(2)−S(2)	85.07(4)
S(2)−Fe(1)−Fe(2)	56.45(3)	S(1)−Fe(2)−Fe(1)	56.04(3)
Fe(1)−S(1)−Fe(2)	67.62(3)	C(9)−C(8)−C(7)	114.5(3)
		3	
Fe(1)−S(1)	2.2549(6)	Fe(2)−S(2)	2.2535(7)
Fe(1)−S(2)	2.2609(7)	O(7)−C(8)	1.469(2)
Fe(1)−Fe(2)	2.5088(5)	O(7)−C(10)	1.349(2)
Fe(2)−S(1)	2.2517(7)	O(8)−C(10)	1.207(2)
S(2)−Fe(1)−S(1)	85.00(2)	S(2)−Fe(1)−Fe(2)	56.097(19)
S(1)−Fe(2)−Fe(1)	56.232(17)	S(1)−Fe(1)−Fe(2)	56.112(19)
S(2)−Fe(2)−Fe(1)	56.380(19)	S(2)−Fe(2)−S(1)	85.25(2)
Fe(2)−S(1)−Fe(1)	67.656(18)	C(8)−O(7)−C(10)	116.51(14)
		4	
Fe(1)−S(1)	2.2495(5)	Fe(2)−S(2)	2.2614(5)
Fe(1)−S(2)	2.2467(5)	O(7)−C(8)	1.4600(17)
Fe(1)−Fe(2)	2.5028(4)	O(7)−C(10)	1.3528(18)
Fe(2)−S(1)	2.2517(5)	O(8)−C(10)	1.1996(18)
S(2)−Fe(1)−S(1)	85.672(15)	S(2)−Fe(2)−Fe(1)	55.999(14)
S(2)−Fe(1)−Fe(2)	56.557(12)	Fe(2)−S(1)−Fe(1)	67.562(15)
S(1)−Fe(1)−Fe(2)	56.262(13)	Fe(1)−S(2)−Fe(2)	67.444(14)
S(1)−Fe(2)−S(2)	85.274(16)	C(8)−O(7)−C(10)	116.25(12)

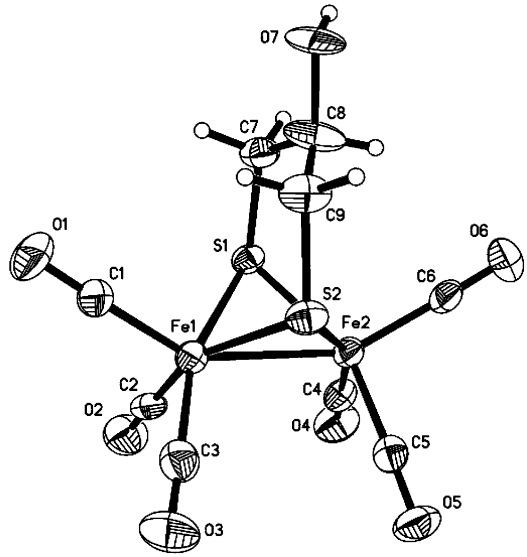

Figure 1. Molecular structure of **A** with 30% probability level ellipsoids.

Complexes **5**−**8** are red solids and have been characterized by elemental analysis, spectroscopy, and X-ray crystallography. The IR spectra of **5**−**8** displayed three to five absorption bands in the region 2077−1934 cm^{-1} for their terminal carbonyls, and **8** exhibited an additional band at 1700 cm^{-1} for its bridgehead C=O functionality. The ^{1}H NMR spectra of **5**−**7** showed two doublets at approximately

(33) Dess, D. B.; Martin, J. C. *J. Org. Chem.* **1983**, *48*, 4155.

Scheme 3

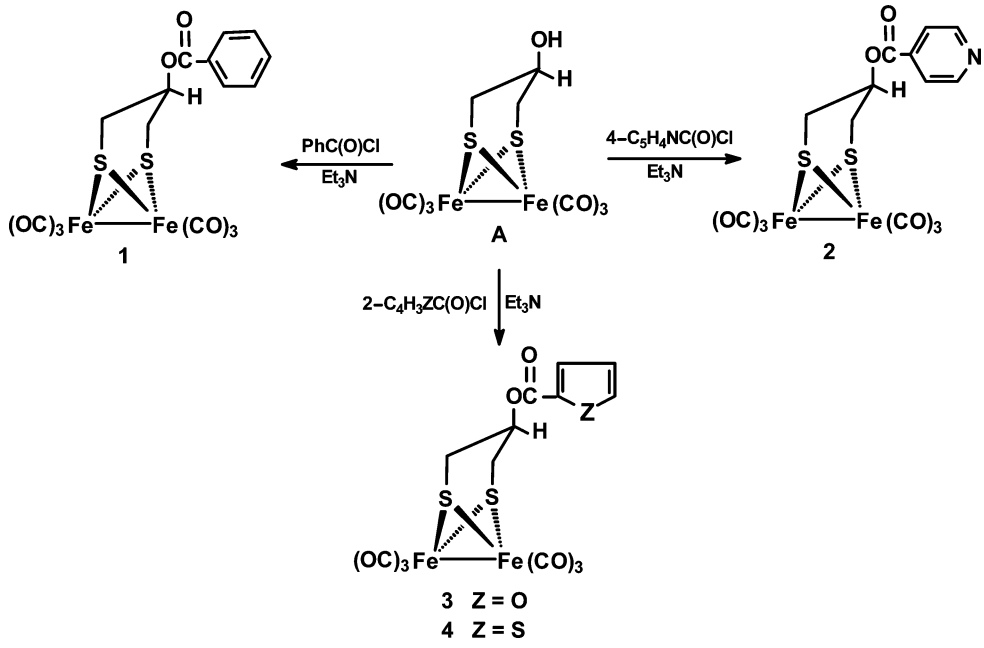

2.0 and 2.8 ppm for the axial and equatorial hydrogen atoms in their two CH_2S groups, whereas the spectrum of **8** displayed only one singlet at 2.86 ppm for the hydrogen atoms in its two CH_2S groups because of rapid folding of the two fused six-membered FeS_2C_3 rings.[24] In addition, the ^{31}P NMR spectra of **5**−**7** showed a singlet in the range 158−198 ppm for their P atoms coordinated to one Fe atom of the diiron subsite.

X-ray crystallography (Figures 5–8 and Table 2) reveals that (i) the structures of **5**−**7** are very similar to each other, with all containing a phosphite-functionalized PDT ligand attached to $Fe(CO)_3$ and $Fe(CO)_2$ units to form three six-membered rings; (ii) the hydrogen atoms attached to the bridgehead C atoms of **5**−**7**, in contrast to those of **A**, **1**, **3**, and **4**, are in an equatorial position due to formation of the P−Fe bond-containing six-membered heterocycles; (iii) in contrast to **A**, **1**, and **3**−**7**, complex **8** has no hydrogen atom attached to its bridgehead C atom, but instead, one oxygen atom is double-bonded to its bridgehead C to form a ketone carbonyl C8═O7 (1.214 Å); and (iv) the Fe−Fe bond lengths of **5**−**8** (2.4929−2.5336 Å) are very close to those of **A**, **1**, **3**, and **4** but are somewhat shorter than those of the natural enzymes (2.55−2.62 Å).[9–11] It is worth pointing out that the [2Fe2SP] models **5**−**7** are structurally very similar to the [2Fe3S] model complexes reported by Pickett and Rauchfuss.[17,23]

Electrochemical Properties of 3, 4, and 8 and Electrocatalytic H_2 Production Catalyzed by 8. The electrochemical properties of **3**, **4**, and **8** were investigated by cyclic voltammetry (CV) in MeCN under CO atmosphere. Table 3 lists their electrochemical data, whereas Figure 9 shows their

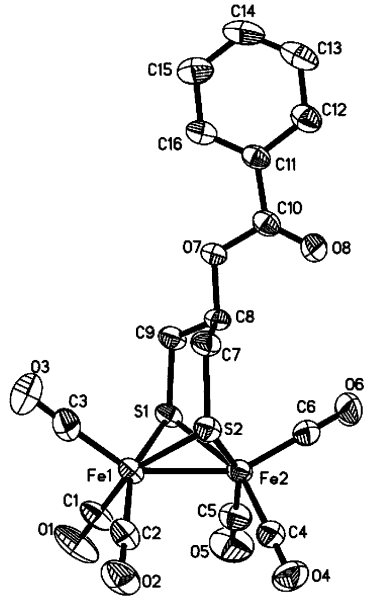

Figure 2. Molecular structure of **1** with 30% probability level ellipsoids.

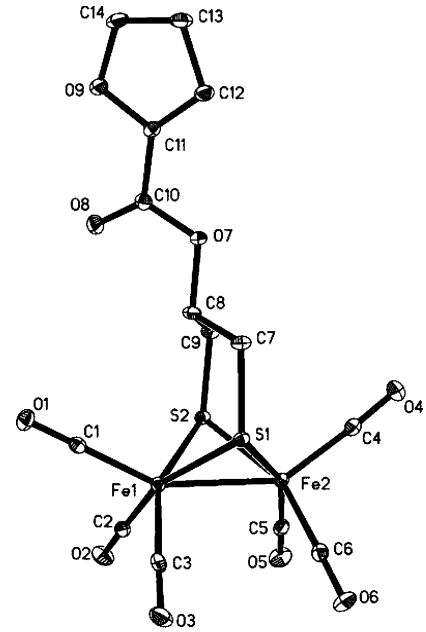

Figure 3. Molecular structure of **3** with 30% probability level ellipsoids.

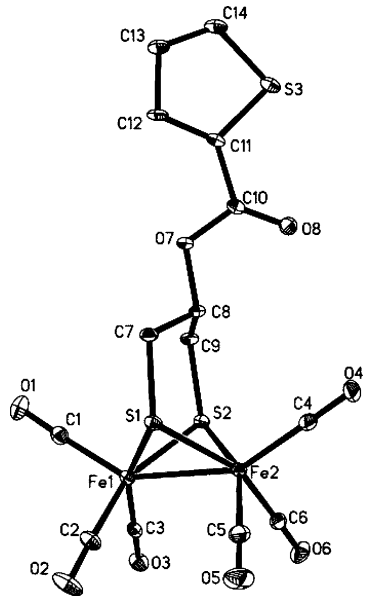

Figure 4. Molecular structure of **4** with 30% probability level ellipsoids.

cyclic voltammograms. It is shown that the first reductions of the three models ($E_{pc} = -1.52$ to -1.59 V) are irreversible one-electron processes, which could be attributed to the Fe^IFe^I/Fe^IFe^0 couple. The second reductions of the three models ($E_{pc} = -2.21$ to -2.39 V) and their oxidations ($E_{pa} = +0.84$ to $+1.01$ V) are also irreversible one-electron processes, which could be ascribed to the Fe^IFe^0/Fe^0Fe^0 and Fe^IFe^I/Fe^IFe^{II} couples, respectively. The one-electron assignments for the aforementioned reduction and oxidation processes were supported by the calculated value of 0.95 faraday/equiv (obtained through the study of the bulk electrolysis of a MeCN solution of **8** at -1.71 V) and the calculated value of $(i_p/\nu^{1/2})/(it^{1/2}) = 3.90$ (obtained through the study of CV and chronoamperometry (CA) of **8**).[34] In addition, the irreversible processes were assigned according to the I_{pa}/I_{pc} and ΔE_p (peak to peak separation) values of the corresponding redox events.[34] The cyclic voltammograms of **8** with CF_3CO_2H ($pK_a = 12.7$ in MeCN)[35] are presented in Figure 10, and for comparison, the cyclic voltammogram of **8** without CF_3CO_2H is also included. As shown in Figure 10, upon the first addition of 1 mM CF_3CO_2H to the solution of **8**, the original first reduction peak at -1.52 V considerably increased and continued to grow up with sequential addition of the acid. Apparently, this features an electrocatalytic proton reduction process.[20,25,36–38] This electrocatalytic H_2 production was further proved by the bulk electrolysis of a MeCN solution of **8** (0.5 mM) with CF_3CO_2H (25 mM) at -1.80 V. During 0.5 h of the bulk electrolysis, 13.5 F per mole of **8** were passed, which corresponds to 6.7 turnovers. In such a large-scale experiment, H_2 bubbles are evident. Gas chromatography (GC) analysis showed that the hydrogen yield was >90%.

Conclusion

On the basis of preparing known complex **A** by a convenient new method, we have synthesized a series of C-functionalized PDT-type models (**1**−**8**) by functional transformation reactions of complex **A**. While **1**−**4** are the C-functionalized models bearing different aromatic carboxylate functionalities, **5**−**7** contain different C-phosphite moieties concurrently coordinated via their P atoms to one Fe atom of their diiron subsites. The simplest one of this series, namely **8**, is the bridgehead ketone derivative of complex **A**. All the new model complexes have been characterized by elemental analysis and spectroscopy, as well as, for starting complex **A** and model complexes **1** and **3**−**8**, by X-ray diffraction analyses. Model **8** is found to be a catalyst for proton reduction to H_2 under electrochemical conditions. It is interesting to note that the phosphite-containing [2Fe2SP] model complexes **5**−**7** are structurally very similar to those [2Fe3S] models previously reported by the Pickett and Rauchfuss groups.[17,23]

Experimental Section

General Comments. All reactions were performed using standard Schlenk and vacuum-line techniques under N_2 atmosphere.

Scheme 4

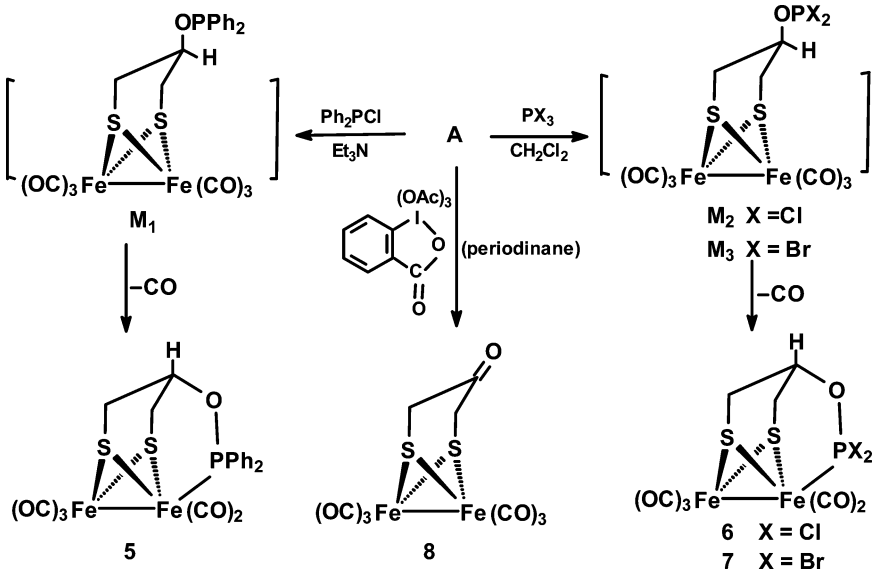

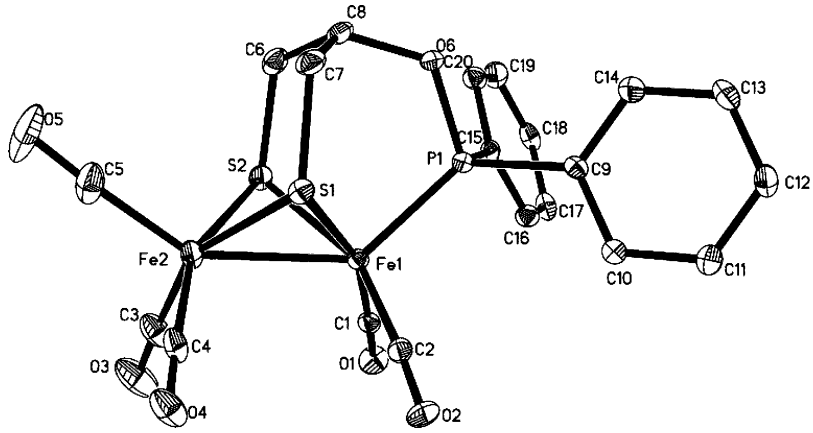

Figure 5. Molecular structure of **5** with 30% probability level ellipsoids.

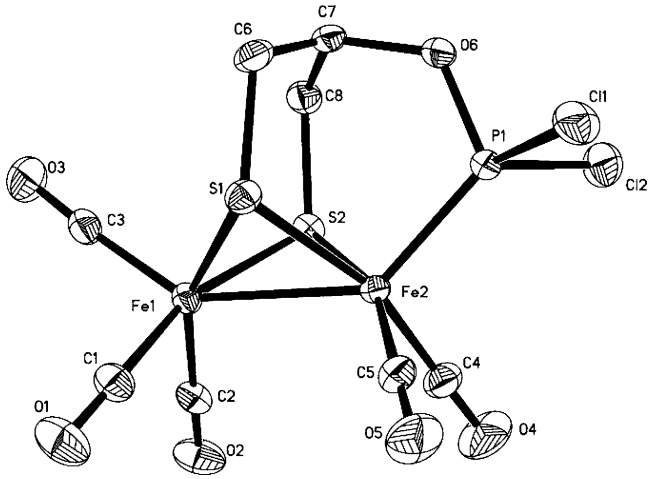

Figure 6. Molecular structure of **6** with 30% probability level ellipsoids.

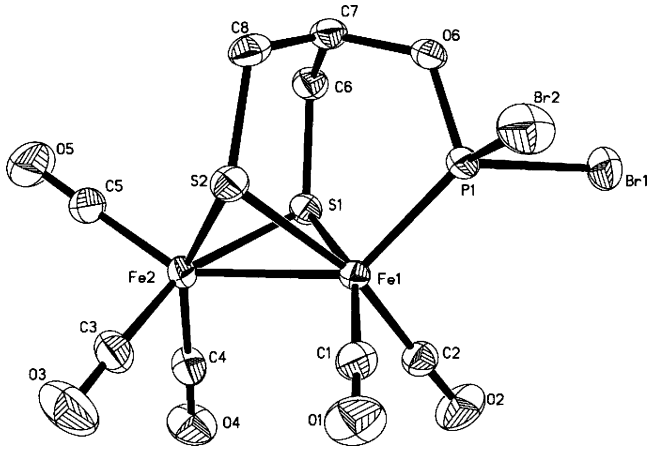

Figure 7. Molecular structure of **7** with 30% probability level ellipsoids.

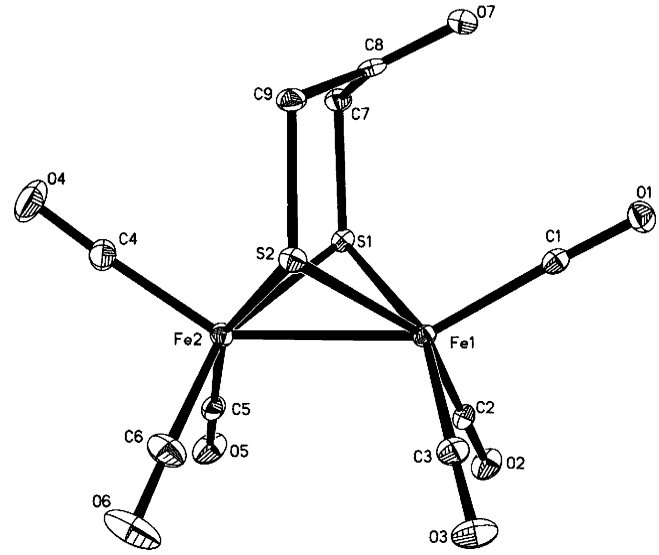

Figure 8. Molecular structure of **8** with 30% probability level ellipsoids.

Dichloromethane and THF were distilled over CaH_2 and sodium/benzophenone ketyl under N_2, respectively. $(BrCH_2)_2CHOH$ (85%, $d = 2.13$), Et_3BHLi (1 M in THF), $PhC(O)Cl$, Ph_2PCl, PCl_3, PBr_3, and triethylamine were available commercially and used as received. $(\mu\text{-}S)_2Fe_2(CO)_6$,[39] 4-$C_5H_4NC(O)Cl\cdot HCl$,[40] furancarbonyl chloride (2-$C_4H_3OC(O)Cl$),[41] thiophenecarbonyl chloride (2-$C_4H_3SC(O)Cl$),[42] and Dess−Martin reagent (periodinane)[43] were prepared according to the literature procedures. Preparative thin-layer chromatography (TLC) was carried out on glass plates ($26 \times 20 \times 0.25$ cm^3) coated with silica gel G (10−40 μm). IR spectra were recorded on a Bio-Rad FTS 6000 spectrophotometer. ^1H NMR and ^{31}P NMR spectra were obtained on a Bruker Avance 300 or a Varian Mercury Plus 400 spectrometer. Elemental analyses were performed on an Elementar Vario EL analyzer. Melting points were determined on a Yanaco MP-500 apparatus and were uncorrected.

Preparation of $[(\mu\text{-}SCH_2)_2CH(OH)]Fe_2(CO)_6$ (A). A red solution of $(\mu\text{-}S)_2Fe_2(CO)_6$ (0.172 g, 0.50 mmol) in THF (10 mL) was

(34) Zanello, P. *Inorganic Electrochemistry. Theory, Practice and Application*; Thomas Graham House: Cambridge, U.K., 2003.
(35) Izutsu, K. *Acid-Base Dissociation Constants in Dipolar Aprotic Solvents*; Blackwell Scientific Publications: Oxford, U.K., 1990.
(36) Chong, D.; Georgakaki, I. P.; Mejia-Rodriguez, R.; Sanabria-Chinchilla, J.; Soriaga, M. P.; Darensbourg, M. Y. *Dalton Trans.* **2003**, 4158.
(37) Mejia-Rodriguez, R.; Chong, D.; Reibenspies, J. H.; Soriaga, M. P.; Darensbourg, M. Y. *J. Am. Chem. Soc.* **2004**, *126*, 12004.
(38) Bhugun, I.; Lexa, D.; Savéant, J.-M. *J. Am. Chem. Soc.* **1996**, *118*, 3982.
(39) Seyferth, D.; Henderson, R. S.; Song, L.-C. *Organometallics* **1982**, *1*, 125.
(40) Meyers, A. I.; Gabel, R. A. *J. Org. Chem.* **1982**, *47*, 2633.
(41) Chadwick, D. J.; McKnight, M. V.; Ngochindo, R. *J. Chem. Soc., Perkin Trans. 1* **1982**, 1343.
(42) Carpenter, A. J.; Chadwick, D. J. *J. Chem. Soc., Perkin Trans. 1* **1985**, 173.
(43) Hart, D. S. *Organic Syntheses*; Wiley: Hoboken, NJ, 2004; Vol. *10*, p 696.

Table 2. Selected Bond Lengths (Å) and Angles (deg) for **5**−**8**

		5	
Fe(1)−S(2)	2.2479(12)	P(1)−O(6)	1.621(3)
Fe(1)−Fe(2)	2.4929(9)	Fe(1)−P(1)	2.1751(13)
Fe(2)−S(1)	2.2596(13)	P(1)−C(9)	1.821(4)
Fe(1)−S(1)	2.2560(13)	P(1)−C(15)	1.820(4)
S(2)−Fe(1)−S(1)	86.55(4)	S(2)−Fe(1)−Fe(2)	56.66(3)
S(1)−Fe(2)−Fe(1)	56.42(4)	S(1)−Fe(1)−Fe(2)	56.56(3)
S(2)−Fe(2)−Fe(1)	56.20(3)	S(2)−Fe(2)−S(1)	86.18(5)
Fe(2)−S(1)−Fe(1)	67.02(4)	P(1)−Fe(1)−S(1)	95.16(4)
		6	
Fe(1)−S(1)	2.2533(10)	Fe(2)−S(2)	2.2517(9)
Fe(1)−S(2)	2.2519(10)	P(1)−O(6)	1.6037(17)
Fe(1)−Fe(2)	2.5336(8)	Fe(2)−P(1)	2.1160(11)
Fe(2)−S(1)	2.2542(9)	P(1)−Cl(1)	2.0411(11)
S(1)−Fe(1)−S(2)	86.46(4)	S(2)−Fe(1)−Fe(2)	55.76(3)
S(1)−Fe(2)−Fe(1)	55.78(3)	S(1)−Fe(1)−Fe(2)	55.82(2)
S(2)−Fe(2)−Fe(1)	55.77(2)	S(1)−Fe(2)−S(2)	86.44(4)
Fe(2)−S(1)−Fe(1)	68.40(3)	P(1)−Fe(2)−Fe(1)	134.27(3)
		7	
Fe(1)−S(1)	2.2423(15)	Fe(2)−S(2)	2.2401(16)
Fe(1)−S(2)	2.2435(15)	P(1)−O(6)	1.594(4)
Fe(1)−Fe(2)	2.5125(11)	Fe(1)−P(1)	2.1072(16)
Fe(2)−S(1)	2.2420(16)	Br(1)−P(1)	2.2154(16)
S(1)−Fe(1)−S(2)	85.86(6)	S(2)−Fe(2)−Fe(1)	55.98(4)
S(1)−Fe(1)−Fe(2)	55.92(4)	S(1)−Fe(2)−S(2)	85.95(6)
S(2)−Fe(1)−Fe(2)	55.85(4)	Fe(1)−S(1)−Fe(2)	68.15(5)
S(2)−Fe(2)−S(1)	85.95(6)	P(1)−Fe(1)−S(2)	91.23(6)
		8	
Fe(1)−S(1)	2.2443(7)	Fe(2)−S(2)	2.2455(7)
Fe(1)−S(2)	2.2554(7)	C(7)−C(8)	1.502(3)
Fe(1)−Fe(2)	2.5192(6)	C(8)−C(9)	1.497(3)
Fe(2)−S(1)	2.2359(7)	O(7)−C(8)	1.214(3)
S(1)−Fe(1)−S(2)	85.58(2)	S(1)−Fe(2)−Fe(1)	55.945(19)
S(1)−Fe(1)−Fe(2)	55.63(2)	S(2)−Fe(2)−Fe(1)	56.150(19)
S(2)−Fe(1)−Fe(2)	55.778(19)	Fe(2)−S(1)−Fe(1)	68.43(2)
S(1)−Fe(2)−S(2)	86.01(2)	C(9)−C(8)−C(7)	116.5(2)

Table 3. Electrochemical Data of **3**, **4**, and **8**[a]

compd	E_{pc} (V) Fe^IFe^I/Fe^IFe^0	E_{pc} (V) Fe^IFe^0/Fe^0Fe^0	E_{pa} (V) Fe^IFe^I/Fe^IFe^{II}
3	−1.58	−2.21	+0.85
4	−1.59	−2.23	+0.84
8	−1.52	−2.39	+1.01

[a] All potentials are versus Fc/Fc^+ in 0.1 M n-Bu_4NPF_6/MeCN.

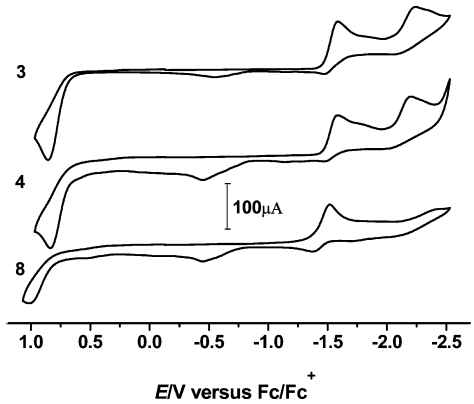

Figure 9. Cyclic voltammograms of **3**, **4**, and **8** (1.0 mM) in 0.1 M n-Bu_4NPF_6/MeCN at a scan rate of 100 mV s^{-1}.

cooled to −78 °C and then treated dropwise with Et_3BHLi (1.0 mL, 1.0 mmol) to give a green solution. After stirring for 15 min, 1,3-dibromo-2-propanol (0.06 mL, 0.50 mmol) was added. The mixture was allowed to warm to room temperature and was stirred at this temperature for 2 h. Volatiles were removed under vacuum, and the residue was subjected to TLC using CH_2Cl_2/petroleum ether

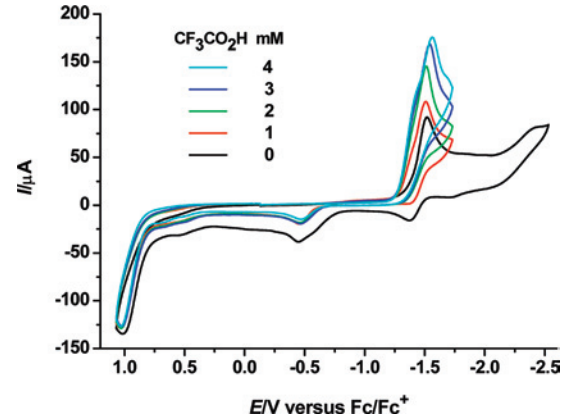

Figure 10. Cyclic voltammograms of **8** (1.0 mM) with CF_3CO_2H (0−4 mM) in 0.1 M n-Bu_4NPF_6/MeCN at a scan rate of 100 mV s^{-1}.

(v/v = 3:1) as eluent. From the major red band, **A** was obtained as a red solid (0.085 g, 42%), mp 102−104 °C. Anal. Calcd for $C_9H_6Fe_2O_7S_2$: C, 26.89; H, 1.50. Found: C, 26.79; H, 1.33. IR (KBr disk): $\nu_{C\equiv O}$ 2078 (s), 2036 (vs), 2009 (vs), 1990 (vs), 1973 (vs); ν_{O-H} 3302 (m) cm^{-1}. ^1H NMR (300 MHz, $CDCl_3$): 1.50 (t, $2H_a$, $J_{HaHe} = J_{HaHa'} = 12.0$ Hz), 1.79 (br s, 1H, OH), 2.79 (dd, 2He, $J_{HeHa} = 12.9$ Hz, $J_{HeHa'} = 3.9$ Hz), 3.06−3.17 (m, $1H_{a'}$) ppm (In this paper H_a and H_e denote the axially and equatorially bonded H atoms in CH_2S groups, while $H_{a'}$ and $H_{e'}$ represent those axially or equatorially bonded to the bridgehead C atom).

Preparation of [(μ-SCH$_2$)$_2$CHO$_2$CPh]Fe$_2$(CO)$_6$ (1). To a solution of **A** (0.200 g, 0.50 mmol) in CH_2Cl_2 (20 mL) cooled to 0 °C were added PhC(O)Cl (0.11 mL, 1.0 mmol) and Et_3N (0.14 mL, 1.0 mmol). The mixture was allowed to warm to room temperature and was stirred at this temperature for 2 h. Volatiles were removed under vacuum, and the residue was subjected to TLC using CH_2Cl_2/petroleum ether (v/v = 2:3) as eluent. From the main red band, **1** was obtained as a red solid (0.160 g, 63%), mp 128−130 °C. Anal. Calcd for $C_{16}H_{10}Fe_2O_8S_2$: C, 37.97; H, 1.99. Found: C, 38.11; H, 2.08. IR (KBr disk): $\nu_{C\equiv O}$ 2073 (s), 2037 (vs), 2003 (vs), 1984 (vs), 1973 (s); $\nu_{C=O}$ 1726 (s) cm^{-1}. ^1H NMR (400 MHz, $CDCl_3$): 1.70 (t, $2H_a$, $J_{HaHe} = J_{HaHa'} = 12.4$ Hz), 2.93 (dd, $2H_e$, $J_{HeHa} = 12.8$ Hz, $J_{HeHa'} = 4.4$ Hz), 4.38−4.60 (m, $1H_{a'}$), 7.40−7.95 (m, 5H, C_6H_5) ppm.

Preparation of [(μ-SCH$_2$)$_2$CHO$_2$CC$_5$H$_4$N-4]Fe$_2$(CO)$_6$ (2). The same procedure was followed as that for the preparation of **1**, but 4-$C_5H_4NC(O)Cl\cdot HCl$ (0.180 g, 1.0 mmol), Et_3N (0.28 mL, 2.0 mmol), and CH_2Cl_2/acetone (v/v = 100:1) were used in place of the corresponding materials. From the major red band, **2** was obtained as a red solid (0.154 g, 61%), mp 188−190 °C. Anal. Calcd for $C_{15}H_9Fe_2NO_8S_2$: C, 35.53; H, 1.79; N, 2.76. Found: C, 35.52; H, 1.89; N, 2.83. IR (KBr disk): $\nu_{C\equiv O}$ 2073 (s), 2038 (vs), 2012 (vs), 1992 (vs), 1978 (s); $\nu_{C=O}$ 1733 (s) cm^{-1}. ^1H NMR (400 MHz, $CDCl_3$): 1.71 (t, $2H_a$, $J_{HaHe} = J_{HaHa'} = 12.4$ Hz), 2.92 (dd, $2H_e$, $J_{HeHa} = 12.8$ Hz, $J_{HeHa'} = 4.0$ Hz), 4.40−4.58 (m, $1H_{a'}$), 8.36, 10.74 (2 br s, 4H, C_5H_4N) ppm.

Preparation of [(μ-SCH$_2$)$_2$CHO$_2$CC$_4$H$_3$O-2]Fe$_2$(CO)$_6$ (3). A solution of **A** (0.140 g, 0.35 mmol), 2-$C_4H_3OC(O)Cl$ (0.40 mL, 4.1 mmol), and Et_3N (0.70 mL, 5.0 mmol) in CH_2Cl_2 (10 mL) was stirred at room temperature for 5 h. After removal of volatiles, the residue was subjected to TLC using acetone/petroleum ether (v/v = 1:2) as eluent. From the major red band, **3** was obtained as a red solid (0.120 g, 70%), mp 112−114 °C. Anal. Calcd for $C_{14}H_8Fe_2O_9S_2$: C, 33.90; H, 1.63. Found: C, 33.80; H, 1.84. IR (KBr disk): $\nu_{C\equiv O}$ 2076 (s), 2035 (vs), 1997 (vs), 1979 (vs),1961 (s), 1937 (m); $\nu_{C=O}$ 1735 (s) cm^{-1}. ^1H NMR (300 MHz, $CDCl_3$):

Table 4. Crystal Data and Structure Refinement Details for **A**, **1**, **3**, and **4**

	A	1	3	4
mol formula	2 ($C_9H_6Fe_2O_7S_2$) $CHCl_3$	$C_{16}H_{10}Fe_2O_8S_2$	$C_{14}H_8Fe_2O_9S_2$	$C_{14}H_8Fe_2O_8S_3$
mol wt	923.28	506.06	496.02	512.08
cryst syst	monoclinic	monoclinic	triclinic	monoclinic
space group	*P*2(1)/*n*	*P*2(1)/*c*	$P\bar{1}$	*P*121/*c*1
a/Å	15.122(4)	13.802(3)	8.7846 (16)	13.5497(17)
b/Å	6.9241(18)	8.4531(17)	9.121(2)	8.2687(10)
c/Å	32.378(9)	17.059(4)	11.778(3)	16.800(3)
α/deg	90	90	78.677(8)	90
β/deg	99.132(5)	96.649(4)	79.185(10)	98.085(5)
γ/deg	90	90	76.766(10)	90
V/Å^3	3347.2(15)	1977.0(7)	890.7(3)	1863.5(4)
Z	4	4	2	4
D_c/g cm^{-3}	1.832	1.700	1.850	1.825
abs coeff/mm^{-1}	2.247	1.719	1.909	1.932
F(000)	1832	1016	496	1024
index ranges	$-9 \le h \le 18$	$-17 \le h \le 13$	$-11 \le h \le 9$	$-15 \le h \le 18$
	$-8 \le k \le 8$	$-9 \le k \le 10$	$-11 \le k \le 11$	$-11 \le k \le 10$
	$-40 \le l \le 37$	$-21 \le l \le 17$	$-15 \le l \le 15$	$-22 \le l \le 22$
rflns	18218	10846	8309	17664
indep rflns	6892	4030	4155	4791
$2\theta_{max}$/deg	53.06	52.84	55.70	57.46
R	0.0556	0.0386	0.0250	0.0245
R_w	0.0679	0.0641	0.0616	0.0575
GOF	0.981	1.044	0.964	0.998
largest diff peak and hole/e Å^{-3}	0.451/−0.427	0.279/−0.351	0.437/−0.406	0.335/−0.375

Table 5. Crystal Data and Structure Refinement Details for **5**−**8**

	5	6	7	8
mol formula	$C_{20}H_{15}Fe_2O_6PS_2$	$C_8H_5Cl_2Fe_2O_6PS_2$	$C_8H_5Br_2Fe_2O_6PS_2$	$C_9H_4Fe_2O_7S_2$
mol wt	558.11	474.81	563.73	399.94
cryst syst	monoclinic	monoclinic	monoclinic	monoclinic
space group	*P*121/*a*1	*P*2(1)/*n*	*P*2(1)/*c*	*P*121/*n*1
a/Å	11.799(3)	6.619(3)	13.127(3)	17.259(3)
b/Å	17.254(4)	14.745(6)	10.202(2)	8.8183(12)
c/Å	12.113(3)	16.380(7)	12.752(3)	18.165(3)
α/deg	90	90	90	90
β/deg	115.785(4)	99.272(7)	107.935(4)	100.805(2)
γ/deg	90	90	90	90
V/Å^3	2220.4(10)	1577.6(12)	1624.7(6)	2715.7(7)
Z	4	4	4	8
D_c/g cm^{-3}	1.670	1.999	2.305	1.956
abs coeff/mm^{-1}	1.601	2.561	7.077	2.468
F(000)	1128	936	1080	1584
index ranges	$-15 \le h \le 15$	$-8 \le h \le 3$	$-16 \le h \le 15$	$-22 \le h \le 22$
	$-22 \le k \le 22$	$-18 \le k \le 18$	$-12 \le k \le 12$	$-11 \le k \le 8$
	$-15 \le l \le 15$	$-20 \le l \le 20$	$-8 \le l \le 15$	$-23 \le l \le 23$
rflns	27647	8957	9103	25097
indep rflns	5293	3221	3315	6482
$2\theta_{max}$ /deg	55.76	52.72	52.80	55.78
R	0.0672	0.0260	0.0401	0.0293
R_w	0.1365	0.0595	0.0848	0.0715
GOF	1.188	1.062	0.989	1.071
largest diff peak and hole/e Å^{-3}	0.566/−0.626	0.310/−0.484	0.749/−0.415	0.401/−0.423

1.72 (t, 2H$_a$, $J_{HaHe} = J_{HaHa'} = 11.7$ Hz), 2.90 (dd, 2H$_e$, $J_{HeHa} = 12.0$ Hz, $J_{HeHa'} = 3.0$ Hz), 4.51 (br s, 1H$_{a'}$), 6.51, 7.16, 7.57 (3s, 3H, C_4H_3O) ppm.

Preparation of [(*μ*-SCH$_2$)$_2$CHO$_2$CC$_4$H$_3$S-2]Fe$_2$(CO)$_6$ (4). The same procedure was followed as that for the preparation of **3**, but 2-$C_4H_3SC(O)Cl$ (0.44 mL, 4.1 mmol) was used instead of 2-$C_4H_3OC(O)Cl$. **4** was obtained as a red solid (0.103 g, 58%), mp 116−118 °C. Anal. Calcd for $C_{14}H_8Fe_2O_8S_3$: C, 32.84; H, 1.57. Found: C, 33.08; H, 1.38. IR (KBr disk): $\nu_{C\equiv O}$ 2073 (s), 2036 (vs), 2001 (vs), 1981 (vs), 1948 (s); $\nu_{C=O}$ 1718 (s) cm^{-1}. ^{1}H NMR (300 MHz, $CDCl_3$): 1.69 (t, 2H$_a$, $J_{HaHe} = J_{HaHa''} = 11.4$ Hz), 2.92 (d, 2H$_e$, $J_{HeHa} = 11.1$ Hz), 4.44 (br s, 1H$_{a'}$), 7.09, 7.58, 7.75 (3s, 3H, C_4H_3S) ppm.

Preparation of [(*μ*-SCH$_2$)$_2$CHOPPh$_2$-*η*^{1}]Fe$_2$(CO)$_5$ (5). To a solution of **A** (0.100 g, 0.25 mmol) in THF (5 mL) cooled to 0 °C were added Et_3N (0.035 mL, 0.25 mmol) and Ph_2PCl (0.05 mL, 0.25 mmol). The new solution was allowed to warm to room temperature and was stirred at this temperature overnight. After removal of volatiles, the residue was subjected to TLC using CH_2Cl_2/petroleum ether (v/v = 1:2) as eluent. From the main red band, **5** was obtained as a red solid (0.067 g, 48%), mp 177−178 °C. Anal. Calcd for $C_{20}H_{15}Fe_2O_6PS_2$: C, 43.04; H, 2.71. Found: C, 43.05; H, 2.87. IR (KBr disk): $\nu_{C\equiv O}$ 2047 (s), 1973 (vs), 1934 (s) cm^{-1}. ^{1}H NMR (400 MHz, $CDCl_3$): 1.94 (d, 2H$_a$, $J_{HaHe} = 14.0$ Hz), 2.65 (d, 2H$_e$, $J_{HeHa} = 14.0$ Hz), 4.98−5.03 (m, 1H$_{e'}$), 7.45−7.73 (m, 10H, $2C_6H_5$) ppm. ^{31}P NMR (162 MHz, $CDCl_3$, 85% H_3PO_4): 158.33 (s) ppm.

Preparation of [(*μ*-SCH$_2$)$_2$CHOPCl$_2$-*η*^{1}]Fe$_2$(CO)$_5$ (6). To a red solution of **A** (0.100 g, 0.25 mmol) in CH_2Cl_2 (10 mL) was added PCl_3 (0.022 mL, 0.25 mmol). The mixture was stirred at room

temperature for 6 h. Volatiles were removed under vacuum, and the residue was subjected to TLC using CH_2Cl_2/petroleum ether (v/v = 1:3) as eluent. From the main red band, **6** was obtained as a red solid (0.088 g, 74%), mp 136−138 °C. Anal. Calcd for $C_8H_5Cl_2Fe_2O_6PS_2$: C, 20.24; H, 1.06. Found: C, 19.98; H, 1.19. IR (KBr disk): $\nu_{C\equiv O}$ 2063 (vs), 2019 (vs), 1992 (vs), 1973 (vs), 1943 (m) cm^{-1}. ^1H NMR (400 MHz, $CDCl_3$): 1.98 (d, $2H_a$, J_{HaHe} = 12.8 Hz), 2.81 (d, $2H_e$, J_{HeHa} = 12.4 Hz), 5.2−5.25 (m,$1H_{e'}$) ppm. ^{31}P NMR (162 MHz, $CDCl_3$, 85% H_3PO_4): 198.00 (s) ppm.

Preparation of [(μ-SCH_2)$_2$CHOPBr_2-η^1]$Fe_2(CO)_5$ (7). The same procedure was followed as that for the preparation of **6**, but PBr_3 (0.024 mL, 0.25 mmol) was used in place of PCl_3, and the mixture was stirred for 4 h. From the main red band, **7** was obtained as a red solid (0.101 g, 72%), mp 122 °C (dec). Anal. Calcd for $C_8H_5Br_2Fe_2O_6PS_2$: C, 17.05; H, 0.89. Found: C, 17.09; H, 0.96. IR (KBr disk): $\nu_{C\equiv O}$ 2057 (vs), 2015 (vs), 1967 (vs). ^1H NMR (300 MHz, $CDCl_3$): 2.01 (d, $2H_a$, J_{HaHe} = 15.0 Hz), 2.90 (d, $2H_e$, J_{HeHa} = 14.5 Hz), 5.20−5.26 (m, $1H_{e'}$) ppm. ^{31}P NMR (162 MHz, $CDCl_3$, 85% H_3PO_4): 162.92 (s) ppm.

Preparation of [(μ-SCH_2)$_2$C=O]$Fe_2(CO)_6$ (8). To a solution of **A** (0.080 g, 0.20 mmol) in CH_2Cl_2 (10 mL) was added Dess−Martin reagent (0.093 g, 0.22 mmol). The mixture was stirred at room temperature for 0.5 h. Volatiles were removed under vacuum, and the residue was subjected to TLC using CH_2Cl_2/petroleum ether (v/v = 1:1) as eluent. From the main red band, **8** was obtained as a red solid (0.032 g, 40%), mp 108−110 °C. Anal. Calcd for $C_9H_4Fe_2O_7S_2$: C, 27.03; H, 1.01. Found: C, 27.11; H, 1.29. IR (KBr disk): $\nu_{C\equiv O}$ 2077 (vs), 2037 (vs), 2001 (vs), 1987 (vs); $\nu_{C=O}$ 1700 (s) cm^{-1}. ^1H NMR (400 MHz, $CDCl_3$): 2.86 (s, 4H, $2CH_2S$) ppm.

X-ray Structure Determinations of A, 1, and 3−8. Single crystals of **A**, **1**, and **3**−**8** suitable for X-ray diffraction analyses were grown by slow evaporation of the CH_2Cl_2/hexane solutions of **1** and **3**−**5** at −10 °C, a $CHCl_3$/hexane solution of **A** at −10 °C, the CH_2Cl_2/ petroleum ether solutions of **6** and **7** at 4 °C, or a CH_2Cl_2/hexane solution of **8** at −20 °C, respectively. A single crystal of **A**, **1**, **6**, or **7** was mounted on a Bruker SMART 1000 diffractometer. Data were collected at room temperature by using a graphite monochromator with Mo Kα radiation (λ = 0.71073 Å) in the ω-$\phi\varphi$ scanning mode. Absorption correction was performed by SADABS program.[44] A single crystal of **3**, **4**, **5**, or **8** was mounted on a Rigaku MM-007 (rotating anode) diffractometer equipped with Saturn 70CCD. Data were collected at room temperature, using a confocal monochromator with Mo Kα radiation (λ = 0.71070 Å) in the ω-ϕ scanning mode. Data collection, reduction, and absorption correction were performed by the CRYSTALCLEAR program.[45] All the structures were solved by direct methods using the SHELXS-97 program[46] and refined by full-matrix least-squares techniques (SHELXL-97)[47] on F^2. Hydrogen atoms were located using the geometric method. The details of crystal data, data collections, and structure refinements of **A**, **1**, **3**, and **4** and **5**−**8** are summarized in Tables 4 and 5, respectively.

Electrochemistry. Acetonitrile (Fisher Chemicals, HPLC grade) was used in the electrochemical experiments. A solution of 0.1 M n-Bu_4NPF_6 in MeCN was used as the electrolyte in all cyclic voltammetric experiments. Electrochemical measurements were made using a BAS Epsilon potentiostat. All voltammograms were obtained in a three-electrode cell with a 3 mm diameter glassy carbon working electrode, a platinum counter electrode, and a Ag/Ag^+ (0.01 M $AgNO_3$/0.1 M n-Bu_4NPF_6 in MeCN) reference electrode under CO atmosphere. The working electrode was polished with 0.05 μm alumina paste and sonicated in water for 10 min prior to use. Bulk electrolysis was run on a vitreous carbon rod (ca. 3 cm^2) in a gastight H-type electrochemical cell containing 20 mL of MeCN. All potentials are quoted against the ferrocene/ferrocenium (Fc/Fc^+) potential. Gas chromatography was performed with a Shimadzu gas chromatograph GC-9A under isothermal conditions with nitrogen as a carrier gas and a thermal conductivity detector.

Acknowledgment. We are grateful to the National Natural Science Foundation of China and to the Specialized Research Fund for the Doctoral Program of Higher Education of China for financial support of this work.

Supporting Information Available: Full tables of crystal data, atomic coordinates, thermal parameters, and bond lengths and angles for **A**, **1**, and **3**−**8** as CIF files. This material is available free of charge via the Internet at http://pubs.acs.org.

IC701982Z

(44) Sheldrick, G. M. *SADABS, A Program for Empirical Absorption Correction of Area Detector Data*; University of Göttingen: Göttingen, Germany, 1996.

(45) *CRYSTALCLEAR 1.3.6.*; Rigaku and Rigaku/MSC: The Woodlands, TX, 2005.

(46) Sheldrick, G. M. *SHELXS97, A Program for Crystal Structure Solution*; University of Göttingen: Göttingen, Germany, 1997.

(47) Sheldrick, G. M. *SHELXL97, A Program for Crystal Structure Refinement*; University of Göttingen: Göttingen, Germany, 1997.